molecular microbiology

Branching and intercellular communication in the Section V cyanobacterium Mastigocladus laminosus, a complex multicellular prokaryote

Journal:	*Molecular Microbiology*
Manuscript ID:	MMI-2013-13810.R1
Manuscript Type:	Research Article
Date Submitted by the Author:	n/a
Complete List of Authors:	Nuernberg, Dennis; Queen Mary University of London, School of Biological and Chemical Sciences Mariscal, Vicente; CSIC, Instituto de Bioquimica Vegetal y Fotosintesis Parker, Jamie; Queen Mary University of London, School of Biological and Chemical Sciences Mastroianni, Giulia; Queen Mary University of London, School of Biological and Chemical Sciences Flores, Enrique; CSIC, Instituto de Bioquimica Vegetal y Fotosintesis Mullineaux, Conrad; Queen Mary University of London, School of Biological and Chemical Sciences
Key Words:	Cyanobacteria, True branching, Mastigocladus laminosus, Intercellular communication, Cell differentiation

Branching and intercellular communication in the Section V cyanobacterium *Mastigocladus laminosus*, a complex multicellular prokaryote

Dennis J Nürnberg[1], Vicente Mariscal[2], Jamie Parker[1], Giulia Mastroianni[1], Enrique Flores[2], and Conrad W Mullineaux[1#]

[1]School of Biological and Chemical Sciences, Queen Mary University of London, Mile End Road, London E1 4NS, United Kingdom

[2]Instituto de Bioquímica Vegetal y Fotosíntesis, Consejo Superior de Investigaciones Científicas and Universidad de Sevilla, Américo Vespucio 49, E-41092 Seville, Spain

[#] For correspondence. E-mail c.mullineaux@qmul.ac.uk; Tel. (+44) 20 7882 3645; Fax (+44) 20 8983 0973.

Running title: Intercellular communication in *Mastigocladus laminosus*

Keywords: cyanobacteria, true branching, *Mastigocladus laminosus*, intercellular communication, SepJ, cell differentiation

Summary

The filamentous Section V cyanobacterium *Mastigocladus laminosus* is one of the most morphologically complex prokaryotes. It exhibits cellular division in multiple planes, resulting in the formation of true branches, and cell differentiation into heterocysts, hormogonia and necridia. Here, we investigate branch formation and intercellular communication in *M. laminosus*. Monitoring of membrane rearrangement suggests that branch formation results from a randomised direction of cell growth. Transmission electron microscopy reveals cell junction structures likely to be involved in intercellular communication. We identify a *sepJ* gene, coding for a potential key protein in intercellular communication, and show that SepJ is localised at the septa. To directly investigate intercellular communication, we loaded the fluorescent tracer 5-carboxyfluorescein diacetate into the cytoplasm, and quantified its intercellular exchange by Fluorescence Recovery after Photobleaching. Results demonstrate connectivity of the main trichome and branches, enabling molecular exchange throughout the filament network. Necridia formation inhibits further molecular exchange, determining the fate of a branch likely to become a hormogonium. Cells in young, narrow trichomes and hormogonia exhibited faster exchange rates than cells in older, wider trichomes. Signal transduction to coordinate movement of hormogonia might be accelerated by reducing cell volume.

Introduction

Among non-eukaryotes, cyanobacteria have achieved a high degree of morphological complexity and diversity. It is remarkable that multicellularity in this phylum evolved early in Earth history, possibly as early as the “Great Oxygenation Event” that took place around 2.48 to 2.32 billion

years ago and allowed the development of all life we know today (Bekker *et al.*, 2004; Tomitani *et al.*, 2006; Konhauser *et al.*, 2011; Schirrmeister *et al.*, 2011). According to their morphology, cyanobacteria have been divided into five sections, including unicellular forms (Section I and II), filamentous (Section III and IV) and filamentous-branching forms (Section V) (Rippka *et al.*, 1979). Organisms of Section IV (also known as order Nostocales (Komárek and Anagnostidis, 1989)) and V (Stigonematales (Anagnostidis and Komárek, 1990)) show additionally the ability to undergo cell differentiation, forming heterocysts (specialised cells for nitrogen fixation), and sometimes also akinetes (resting cells for survival of adverse environmental conditions), and hormogonia (motile filaments for dispersal and symbiosis competence). Accordingly, multicellularity in cyanobacteria has been defined by three processes: cell-cell adhesion, intercellular communication and terminal cell differentiation (Flores and Herrero, 2010).

While our understanding of multicellularity in Section IV has deepened considerably by studying *Anabaena* sp. PCC 7120 as model organism (for review see (Flores and Herrero, 2010)), there is little known about cyanobacteria of Section V. The best understood organism within this section is probably *Mastigocladus laminosus*, which is a major component of epilithic microbial mats at White Creek, Yellowstone National Park, USA (Miller *et al.*, 2006), and can be found in geothermal sites and hot springs worldwide with an upper temperature limit of 63°C (Cohn, 1862; Schwabe, 1960; Castenholz, 1976; Melick *et al.*, 1991; Finsinger *et al.*, 2008; Soe *et al.*, 2011; Mackenzie *et al.*, 2013).

Under most conditions, *M. laminosus* forms a dense network of intertwined narrow and wide trichomes (also known as type II (secondary) and type I (primary) trichomes respectively (Schwabe, 1960)). While cells of narrow trichomes have a uniform cylindrical shape, cells of wide trichomes are rounded and pleomorphic, giving usually rise to true branches, the

characteristic feature for cyanobacteria of Section V (Anagnostidis and Komárek, 1990; Golubić *et al.*, 1996; Komárek *et al.*, 2003). Microfossil records from Rhynie, Aberdeenshire, Scotland support the presence of this complex morphotype already around 400 million years ago (Croft and George, 1959). True branching includes several different types, which have been named for simplicity after their morphological appearance, including "T", "V", "X", and (reverse) "Y" branching (Anagnostidis and Komárek, 1990; Golubić *et al.*, 1996). Lateral "T", "V" and (reverse) "Y" branches are comprised of cylindrical cells (Desikachary, 1959; Fogg *et al.*, 1973; Golubić *et al.*, 1996). Branches can differentiate into motile hormogonia which are released from the main filament by death and disintegration of the branching point (Balkwill *et al.*, 1984). The released hormogonia glide away from the parental colony, and finally form new colonies by differentiating into spherical cells, which give rise to new lateral branches (Hernandez-Muniz and Stevens, 1987; Robinson *et al.*, 2007). According to ultrastructural investigations, cell division in *M. laminosus* and *Fischerella ambigua* differs from that seen in filamentous cyanobacteria of Sections III and IV (Thurston and Ingram, 1971; Martin and Wyatt, 1974; Nierzwicki *et al.*, 1982). Rounded cells in wide trichomes were suggested to be separated by their surrounding sheath (Martin and Wyatt, 1974). This would suggest that their filamentous character is only maintained by sheath material, so cyanobacteria of Section V may not represent the pinnacle of development among cyanobacteria but rather a primitive and basic form linking coccoid and filamentous forms (Martin and Wyatt, 1974). Under nitrogen deprivation almost every cell can differentiate into a heterocyst, following no regular spacing pattern, often forming multiple contiguous heterocysts in wide trichomes (MCH; sets of heterocysts, connected to each other without vegetative cells in between) (Nierzwicki-Bauer *et al.*, 1984a; Nierzwicki-Bauer *et al.*, 1984b; Stevens *et al.*, 1985). This raises the question of how cells communicate in *M. laminosus*.

Here we investigate intercellular communication in *M. laminosus* by loading the fluorescent tracer 5-carboxyfluorescein diacetate (5-CFDA) into the cytoplasm, and performing Fluorescence Recovery after Photobleaching (FRAP) experiments to observe intercellular exchange of dye molecules, using methodology previously applied to filamentous cyanobacteria of Sections III and IV (Mullineaux *et al.*, 2008). In the Section IV cyanobacterium *Anabaena* sp. PCC7120, there is rapid diffusion of dye molecules between the cytoplasms of neighbouring cells, dependent on the septum-localised proteins SepJ (FraG), FraC and FraD (Mullineaux *et al.*, 2008; Merino-Puerto *et al.*, 2011). Here, we address the questions of whether the branch and the main trichome communicate in *M. laminosus*, and whether exchange depends on the cell morphotype. Our results demonstrate that branch and main trichome exchange molecules, and that exchange depends on the cell morphology, showing that *M. laminosus* makes a particularly complex network of intercellular communication.

Just recently, the genome sequences of several species of Section V were published (Dagan *et al.*, 2013; Shih *et al.*, 2013).It has been suggested that no signature proteins specific to any of the complex morphologies exist (Shih *et al.*, 2013), and that branching might be mainly a result of expressing a very few proteins which affect the regulation of cell division genes and/or the localisation of their proteins (Dagan *et al.*, 2013). Here we follow the localisation of the cytoplasmic membrane during the process of branch formation to gain further insights into this complex event.

Results and Discussion

Randomisation of the axis of growth results in different types of branching

M. laminosus forms two morphologically distinct types of true branches: (reverse) "Y" (Fig. 1A) and "T" branches (Fig. 1B). Both types of branches are not only present in the same culture, but even in the same filament (not shown), raising the question of whether the differences between the two types are merely superficial, or whether they arise from different developmental processes.

We approached this question by visualising the cytoplasmic membrane during branch formation using confocal microscopy and transmission electron microscopy. For confocal microscopy we stained cells with the fluorescent dye FM1-43FX, which highlights the cytoplasmic membrane in cyanobacteria (Schneider *et al.*, 2007). Our results indicate that the (reverse) "Y" and "T" branches are topologically equivalent: in both cases branch formation is initiated by the growth of a cell in a direction other than the main axis of the filament (Fig. 1A,C). This is generally followed by septum formation across the mid-line of the cell, as is the usual rule in bacteria (Fig. 1A). The result of septum formation is that one of the daughter cells is connected to three cells: two in the main trichome and one in the developing branch (Fig. 1A,B). A "T" branch results from cell elongation in a direction roughly perpendicular to the filament axis (Fig. 1B), whereas a (reverse) "Y" branch results from cell elongation at a more acute angle to the filament axis (Fig. 1A,C), but the two cases are only superficially different. This implies that branching is the result of a randomisation of the direction of cell elongation. When cell elongation is constrained to occur along the filament axis, branch formation is repressed. A developmental switch leading to randomisation of the direction of cell elongation allows branches to form. Our conclusion is consistent with the message from recent genome sequence analyses of several cyanobacteria of Section V, which did not detect any specific Section V signature proteins (Dagan *et al.*, 2013; Shih *et al.*, 2013). Furthermore, it was shown by Singh and Tiwari (1969) that true branching can be induced in the non-branching filamentous cyanobacterium *Nostoc linckia* (Roth) Born. et Flah.

(Section IV) by random mutagenesis using ultraviolet irradiation, which implies that branching can be induced by loss of gene function rather than being the result of a complex developmental programme. This fits with our conclusion that branching results from the selective relaxation of a stringent control over the direction of cell elongation. We could detect no obvious patterns in the spacing of branches, which appears to be random. Terminal cells of wide trichomes do not branch and have a different, elongated shape (Fig. 1D), which has been described as a terminal hair (Anagnostidis and Komárek, 1990). The attachment of another cell, or even a cell fragment, at the terminus of the filament is enough to inhibit cell elongation (Fig. S1). A similar topology can be found e.g. in the filamentous cyanobacterium *Oscillatoria acuminate* (Section III; Geitler, 1960).

M. laminosus forms a complex cellular network of communication mediated by septosomes

Until now it has remained unknown whether the branch and the main trichome communicate in cyanobacteria of Section V. A prerequisite for answering this question is to load a hydrophilic fluorescent molecule into the cytoplasm of cells of both the branch and the main trichome. For *Anabaena* sp. PCC 7120 two fluorescent molecules that can be used as tracers have been described in detail, calcein (Mullineaux *et al.*, 2008) and 5-carboxyfluorescein diacetate (5-CFDA; Mariscal *et al.*, 2011). In both cases, the tracer is added to the cell culture in an esterified form which is non-fluorescent and hydrophobic enough to be cell-permeant. Hydrolysis of the ester groups by cytoplasmic esterases converts the molecule to a fluorescent form which is trapped in the cytoplasm because it is too hydrophilic to traverse lipid bilayers. Hence it can be used to probe intercellular exchange of hydrophilic molecules via protein channels at the cell junctions (Mullineaux *et al.*, 2008; Mariscal *et al.*, 2011). We tested both fluorescent tracers for

M. laminosus. The efficiency of cell labelling with 5-CFDA was much higher than that with calcein (data not shown), and hence suitable for further studies.

The question of connectivity between branch and main trichome cannot be answered simply by photobleaching and following fluorescence recovery of the cell at the branch point, as fluorescence recovery might be possible from three directions. We found that branch formation could be induced by agitating the cell culture for 24h in fresh medium, consistent with a previous observation that branch formation is induced by conditions favouring rapid growth (Thurston and Ingram, 1971). Cells were then loaded with 5-CFDA, and fluorescence of entire short branches bleached by scanning the region of the branch at increased laser intensity (Fig. 2). All the cells in a branch, regardless whether they formed a "T" (Fig. 2) or (reverse) "Y" branch (not shown), showed recovery. A quantified analysis of recovery, shown for a specimen "T" branch in Fig. 2, in which the bleached out branch was defined as one region of interest (ROI), reveals that recovery is mediated by cells from both sides next to the branching point. The fluorescence intensity decreases in the adjacent cells over time. Accordingly our results demonstrate that trichomes of *M. laminosus* form a complex interconnected cell communication network. A newly formed branch remains connected to its main trichome.

The exchange of molecules between the cytoplasm of cells requires the presence of cell-to-cell connecting structures penetrating the peptidoglycan layer and the plasma membranes of both cells (e.g. Merino-Puerto *et al.*, 2011; Lehner *et al.*, 2013). The occurrence of such structures, which have been termed septosomes (or microplasmodesmata), has been well characterized in *Anabaena* spp. by various methods, such as thin-section TEM (e.g. Wildon and Mercer, 1963), freeze-fracture EM (Giddings and Staehelin, 1978; Giddings and Staehelin, 1981) and electron tomography (Wilk *et al.*, 2011), but it has remained unclear whether septosomes exist in *M.*

laminosus. A first indication of their presence in *M. laminosus* was given by Marcenko (1962), who could identify pores with an average diameter of 15 nm in the cross-walls of isolated cell wall sacculi. Our electron micrographs of thin sections through the septal regions of *M. laminosus* clearly show structures pervading the septa between vegetative cells (Fig. 3A) and between heterocysts and vegetative cells (Fig. 3B). Different methods of sample preparation for TEM can also be used to reveal insights into the composition of intercellular channels (Wilk *et al.*, 2011). Our results are in good agreement with the proposed proteinaceous nature of the septosomes found in *Anabaena* sp. PCC 7120 (Wilk *et al.*, 2011). While septosomes appear as positively stained structures in a $KMnO_4$-based preparation method (Fig. 3A), they are negatively stained in an OsO_4-based preparation (Fig. 3B).

Although the presence of pores penetrating the septum was shown earlier in *Stigonema hormoides*, *Fischerella muscicola*, and *F. ambigua*, which belong to cyanobacteria of Section V, it has been suggested that these pores do not pierce the underlying plasma membranes, and accordingly do not mediate a direct connection of the protoplasts (Thurston and Ingram, 1971; Butler and Allsopp, 1972). Our results from fluorescent dye exchange, however, show the connectivity of the cytoplasm throughout the entire filament network, which is likely achieved by structures resembling septosomes.

Composition and localisation of SepJ in *M. laminosus* is similar to those found in cyanobacteria of Section IV

Our ultrastructural studies of septa suggest that septosomes consist of proteins. In *Anabaena* sp. PCC 7120 a potential key player is SepJ. SepJ is not only necessary for filament integrity (Nayar *et al.*, 2007; Flores *et al.*, 2007; Merino-Puerto *et al.*, 2010) but also essential for intercellular exchange of molecules (Mullineaux *et al.*, 2008; Mariscal *et al.*, 2011). Although a *sepJ* deletion

196 mutant still exhibits septosomes, the spacing between the two plasma membranes of the
197 neighbouring vegetative cells is significantly reduced (Wilk *et al.*, 2011). We asked whether SepJ
198 is also present in *M. laminosus*. Due to the lack of a genome sequence for this cyanobacterium,
199 we designed primers based on DNA sequence similarity between the *sepJ* and the *hetR* sequences
200 deposited in the GenBank® database (Benson *et al.*, 2011). *hetR* encodes a protein that is a
201 master regulator of heterocyst differentiation in the Section IV cyanobacterium *Anabaena* sp.
202 PCC 7120 (Buikema and Haselkorn, 1991), and is widely distributed among filamentous
203 cyanobacteria, including non-heterocystous species (Zhang *et al.,* 2009). As *hetR* is usually
204 located downstream of *sepJ* we selected a highly conserved region between six cyanobacterial
205 strains of Section V within this gene, and defined it as primer rev_mlam_hetR (Fig. S2A). The
206 design of primer fw_mlam_sepJ was based on an alignment of the *sepJ* sequences from four
207 species, which are filamentous and heterocyst forming (Fig. S2B).

208 The PCR with both primers generated a DNA product that contained a sequence with a high
209 similarity to *sepJ*. The corresponding amino acid sequence revealed that, similar to SepJ from
210 Section IV cyanobacteria (Mariscal *et al.*, 2011), SepJ of *M. laminosus* consists of three domains,
211 including a coiled-coil domain (CC), a highly repetitive linker region (L), and a permease domain
212 (P). To find out whether there exists a correlation between the SepJ domain structure and its
213 distribution among cyanobacteria, we ran a BlastP search with the amino acid sequence of SepJ
214 from *M. laminosus* as query against all cyanobacterial sequences available from the Integrated
215 Microbial Genomes (IMG) database (Markowitz *et al.*, 2012), and against the recently published
216 sequences by Dagan et al. (2013) (April 2013; Table S1). In our analysis we considered proteins
217 which are comprised of either two or three domains ((CC+P) or (CC+L+P)) as SepJ-like proteins,
218 whereas proteins showing only similarity to the permease domain were considered as DME-
219 family permeases. Our analysis revealed that in 62 from 139 cyanobacterial species (45%) a

SepJ-like protein is present, while only 28 cyanobacterial species (20%) possess DME-family permease, of which 16 (12%) can be found additionally in cyanobacteria possessing a SepJ-like protein. While all cyanobacteria of Sections IV and V (20 and 12 species respectively), and most species of Section III (32 from 34 species (94 %)) posses a SepJ-like protein, a SepJ variant is absent from unicellular species of Sections I and II, indicating the importance of SepJ for filamentous cyanobacteria. Furthermore, a closer look at the composition of the SepJ-like proteins in the different cyanobacterial sections reveals that filamentous species of Section III show mainly a two domain protein (CC+P) (23/32 species; 72%), and nearly all filamentous, heterocyst-forming (and branching) cyanobacteria of Sections IV and V exhibit a three-domain (CC+L+P) SepJ variant (20/20 species (100 %); and 11/12 species (92 %) respectively). We conclude that SepJ-like proteins containing a coiled-coil domain and a highly repetitive linker region of various lengths can be attributed to filamentous heterocystous cyanobacteria.

The amino acid sequence of SepJ from *M. laminosus* SAG 4.84 is almost identical to that of *Fischerella muscicola* PCC 7414 (Dagan *et al.*, 2013) despite the great spatial separation of their origins of isolation (Iceland and New Zealand) (Rippka *et al.*, 1979). Intercontinental dispersal e.g. by transpacific winds (Smith *et al.*, 2013) would explain the presence of "similar" strains of *M. laminosus* in such widely separated habitats. A phylogenetic analysis based on 16S rRNA sequences (Fig. S3) strongly supports the close relationship between *F. muscicola* PCC 7414, *M. laminosus* SAG 4.84 and other strains from widely dispersed sites (Table S2). Although the amino acid sequence of SepJ from *M. laminosus* SAG 4.84 and *Fischerella* sp. PCC 7414 show a high similarity, it has to be pointed out that *sepJ* from *Fischerella* sp. PCC 7414 might bear a stop codon in the highly repetitive linker region.

In order to localise SepJ in *M. laminosus* we performed immunofluorescence labelling using the antibody against the coiled-coil domain of SepJ from *Anabaena* sp. PCC 7120 (Mariscal *et al.*, 2011). The experiments show that SepJ is always located in the centre of intercellular septa of *M. laminosus* (Fig. 3C; Fig. S4; Fig. S5). There is also a dispersed background fluorescence signal in the cytoplasm, however this signal is also seen in the absence of the primary anti-SepJ antibody and therefore does not reflect SepJ localisation (Fig. S4). SepJ forms distinct spots not only in the main wide trichome, but also in the narrow branch (Fig. 3C). A newly-formed branching point shows three distinct regions of SepJ located to the adjacent cells (Fig. 3C). The positioning of SepJ likely takes place during the cell division, when the protein forms a ring at the division plane (Fig. S5). These findings are in good agreement with those in *Anabaena* sp. PCC 7120 (Flores *et al.*, 2007) and support the importance of SepJ at the septal region of filamentous, heterocyst-forming cyanobacteria.

Molecular exchange within the filament network is regulated, and depends on cell shape

While branches are comprised of long, narrow, cylindrical cells, main trichomes consist of large, rounded-up cells (e.g. (Schwabe, 1960; Nierzwicki *et al.*, 1982). Although cells in branch and main trichomes show distinct differences in their cell shape, their ultrastructure is similar, varying mainly in the number of carboxysomes and peripherally located lipid bodies. Wide cells possess a higher number of these inclusions than narrow cells (Nierzwicki *et al.*, 1982; Nierzwicki-Bauer *et al.*, 1984b), and it has been suggested that they might be functionally active rather than being in a resting state (Balkwill *et al.*, 1984). To gain further information about the possible function of these different morphotypes, we investigated the ability to exchange molecules by FRAP experiments with the fluorescent tracer 5-CFDA. A parameter to quantify the kinetics of dye exchange between cells is the “exchange coefficient” (E), which can be calculated as previously

described (Mullineaux *et al.*, 2008). E has units of s^{-1} and relates the rate of molecular flux between adjacent cells to the difference in dye concentration between the cells. However, E is not the best parameter to use for making comparisons of the connectivity of morphotypes with significantly different cell volumes, because the concentration changes resulting from flux of molecules across the cell junction depend on cell volume as well as the flux across the junction. Therefore we introduce a new parameter, the "flux coefficient" F, defined as (E x cell volume), with units of $\mu m^3 s^{-1}$. F corrects for the influence of cell volume on E, to give a value that allows comparison of molecular exchange activity at junctions between different morphotypes.

To take the influence of the high degree of cell polymorphism in *M. laminosus* on the cell volume into account, we chose four different geometrical shapes, including cylinder, prolate spheroid, sphere, and oblate spheroid. While cylindrical cells were considered to represent cells in narrow trichomes, both spherical and spheriodal cells were considered to represent cells of wide trichomes. Our results indicate that cells in narrow trichomes exhibit significantly higher E and F values than cells in wide trichomes (Table 1), suggesting that not only the change in concentration of molecules but also the flux of molecules between cells depends on the trichome type. The mechanism which leads to the significant decrease in communication between cells during the process of maturation from a narrow to a wide trichome remains yet to be investigated.

A high degree of cell-cell communication might be essential to ensure a sufficient supply of nutrients and regulators within a fast-growing narrow trichome. To investigate this hypothesis, we considered further cell differentiation processes in *M. laminosus*, which are supposed to require cell-cell communication, including the formation of heterocysts and motile hormogonia.

Nitrogen limitation stimulates extensive heterocyst differentiation in *M. laminosus*. Almost any vegetative cell can differentiate into a heterocyst (Nierzwicki-Bauer *et al.*, 1984b; Stevens *et al.*,

1985). Here we particularly focussed on the localisation of heterocysts in the region of branching. Heterocysts were distinguished from vegetative cells by their diminished pigmentation and the presence of cyanophycin plugs at the cell poles. We observed that any cell in the branching region is capable of undergoing cell differentiation, resulting in the formation of heterocysts in the branching point of a "T"-branch and a (reverse) "Y"-branch (Fig. 4A-D). The position of the cyanophycin plugs in these cells is notable. Heterocysts at the origin of a branch show three cyanophycin plugs, while neighbouring heterocysts in the branching region of "T" and (reverse) "Y"-branches only possess two cyanophycin plugs (Fig. 4B,C). These microscopic observations support our previous FRAP results that *M. laminosus* forms a complex network of various trichome types, which exchange metabolites, including products of nitrogen and carbon fixation. The key function of the main trichomes might be to provide the basis for growth of the organism under favourable environmental conditions.

Earlier observations by Nierzwicki-Bauer *et al*. (1984a) that *M. laminosus* forms multiple contiguous heterocysts in the main trichomes under nitrogen deprivation support this hypothesis. Although we rarely observed the formation of multiple contiguous heterocysts in the main trichome of *M. laminosus* SAG 4.84, we regularly found double heterocysts in the branches (Fig. 4E). It is possible that the different heterocyst localisation is caused either by the altered growth conditions or the diversity of *M. laminosus* strains in general, since a strain of *M. laminosus* Cohn has been described which lacks the ability to form heterocysts (Melick *et al.*, 1991). The formation of double heterocysts is again interesting with regard to the position of cyanophycin plugs. Each heterocyst shows two cyanophycin plugs, resulting in a double cyanophycin plug between both heterocysts (Fig. 4E). Until now the role of cyanophycin (multi-L-arginyl-poly-L-aspartic acid) has remained unclear, though a role as a dynamic nitrogen reserve is likely due to its high nitrogen content of approximately 26% of its mass (Lockau and Ziegler, 2006).

To characterise the heterocyst-heterocyst connection further we used the fluorescent dye FM1-43FX (Schneider *et al.*, 2007). Our results clearly show that both heterocysts are connected via two neck regions (Fig. S6). Overall, heterocysts of *M. laminosus* seem to be much more strongly connected to their neighbouring cells than in *Anabaena* spp. since we never observed any single heterocysts or short filaments with terminal heterocysts.

Another important stage in the life cycle of *M. laminosus* is the formation of hormogonia, motile filaments which glide slowly away from the parental filament, before finally differentiating into a sedentary wide trichome and forming a new colony (Hernandez-Muniz and Stevens, 1987). Hormogonia show a high variability in surface velocity, which differs not only between hormogonia but also for the same hormogonium over time, and a high variability in the directions they move (Hernandez-Muniz and Stevens, 1987). Their ability to reverse the direction of gliding (Hernandez-Muniz and Stevens, 1987) suggests a high degree of cell-cell communication. In order to determine the exchange and flux coefficient for hormogonia we chose to measure the cell dimensions of a moving hormogonium, and correlate them to the tracer exchange data represented earlier. This ensures that also hormogonia are considered which were not moving during the FRAP experiments. As hormogonia are formed by cell division without biomass increase, they can be distinguished from other filament types by their distinctly smaller cell size (Campbell and Meeks, 1989). Accordingly, we defined hormogonia of *M. laminosus* by cell diameter, cell length, and the diameter to length ratio, resulting in a group of cells characterised by an average cell diameter of 2.76 ± 0.31 µm, an average cell length of 3.61 ± 0.88 µm, and a diameter to length ratio of 0.80 ± 0.19 (n=80). While the mean exchange coefficient E is similar to that found between cells in narrow trichomes (E = 0.159 ± 0.072 s^{-1}) and meets the expectation that cellular communication is fast in hormogonia, the flux coefficient F is significantly lower, showing a value similar to that found in wide trichomes (F = 3.60 ± 2.47 μm^3 s^{-1}) (Table 1).

Therefore communication between cells in hormogonia is rapid in the sense that intercellular diffusion of molecules is fast enough to lead to rapid changes in the cytoplasmic concentration of putative signalling molecules. However, as compared to cells in the parental filament, this rapid communication is achieved by reducing the cell volume rather than by accelerating the flux of molecules across the cell junctions. Therefore signal transduction to coordinate movement (and possibly other aspects of the biology) of hormogonia is probably accelerated by the reduction of the cell volume rather than by increased flux of signalling molecules across the cell junctions.

Barriers to cell-cell communication are formed early in the life cycle of *M. laminosus*

The release of a hormogonium from its parental trichome is mediated by the formation of releasing, dead cells, called necridia, which are possibly best studied in *Oscillatoria/Microcoleus* spp. (Kohl, 1903; Lamont, 1969; Brown *et al.*, 2010). Beside heterocysts (Meeks *et al.*, 2002), necridia are one of the few known developmental "dead ends" among prokaryotes, and can be seen as a basic form of programmed cell death (apoptosis). Since a necridium can be found early after the branching event in the growing narrow trichome (Fig. 5A-C), we investigated whether exchange of molecules is still possible between the branch and the main trichome. After loading the fluorescent tracer 5-CFDA into the cytoplasm, we bleached out the fluorescence of the part of the branch which was separated by the necridium and followed its change in fluorescence intensity (Fig. 5A). We did not observe any recovery of the bleached region within 24 s (Fig. 5A) indicating that a necridium inhibits cell-cell communication completely. Accordingly, the fate of a trichome is determined early after branch formation; molecular exchange not being possible once a necridium is formed.

To get an impression of the complexity of this event and its importance for the filamentous network, we investigated the position of necridium formation. Necridia can be easily detected by

359 enhanced red fluorescence in the region of formation, possibly as a result of degradation of the
360 photosynthetic apparatus (Figs. 5B-D and 6A). Necridia also show brighter staining with the
361 membrane dye FM1-43FX (Fig 5B-D), probably because leakiness of the cytoplasmic membrane
362 allows the dye to penetrate to the interior of the cell. We observed that necridia are not only
363 located in the branching point, as reported in an earlier study (Balkwill *et al.*, 1984), but also in
364 various other positions within narrow trichomes, such as the beginning of the recently formed
365 branch (Fig. 5C), indicating that almost any cell within a filament can differentiate into a
366 necridium. Even within the same filament several necridia can be found, contiguous or separated
367 only by a single cell (Fig. 5D), suggesting that necridia formation in *M. laminosus* seems to
368 follow no regular pattern of spacing and distribution.

369

370 The final release of the trichome is a complex mechanism of remodelling the septal region on
371 both sides of the necridium. To avoid cell death of the entire cellular network by efflux of
372 molecules, the membranes of the neighbouring cells have to stay intact, and the channels/pores
373 have to be closed. Electron micrographs confirm that the plasma membrane and outer membrane
374 are sealed at the terminal cell (Fig. 6B). Although we observed that necridia usually consist only
375 of a single cell, they can be formed by two cells (Fig. 5B, D). A possible mechanism to prevent
376 efflux of molecules in other cyanobacteria, e.g. *Symploca muscorum* and *M. vaginatus* might be
377 by the synthesis of an additional cell wall layer at the new terminus ("calyptra"; Pankratz and
378 Bowen, 1963; Lamont, 1969). It remains yet to be investigated whether this structure also exists
379 in *M. laminosus*.

380 Filament breakage, however, is only possible by the disintegration of the membranes of the
381 necridium. To investigate this process we used the cytoplasmic membrane stain FM1-43FX (Fig.

382 5B,C,D) and the DNA stain Hoechst 33258 (Fig. 6A). The fluorescence micrographs indicate that
383 during necridium formation the cytoplasmic membrane of the necridium deteriorates mainly from
384 one terminus of the cell (Fig. 5B,C,D), leaving an "open" and empty (DNA-free) cell attached to
385 the released filament (Fig. 6), while only a small part of membranes remains at the terminus of
386 the parental filament.

387 Concluding remarks

388 Our results demonstrate that *M. laminosus* represents a complex cellular network, in which the
389 main trichome and branches communicate via intercellular connections which resemble
390 septosomes. We observed that exchange between cells within a culture is regulated, depending on
391 cell morphology. Young, narrow trichomes exhibited rapid exchange rates among cells, while
392 old, wide trichomes showed reduced rates. Accordingly, wide trichomes might not only provide a
393 platform for the outgrowth of branches, but they might also support the growth of branches by
394 supplying metabolites in the presence and absence of a combined nitrogen source. Under nitrogen
395 deprivation heterocysts can be found frequently in the branching region, sometimes even in the
396 branching start, forming a heterocyst with three cyanophycin plugs. The integrity of the filament
397 network is only interrupted by the formation of necridia, which inhibit further molecular
398 exchange, and hence determine the fate of a developing branch likely to become a hormogonium,
399 soon after the branching event. Interestingly, signal transduction to coordinate movement of the
400 released hormogonia might be accelerated by the reduction in cell volume.

401 Cell differentiation seems to be generally less regulated than in Section IV cyanobacteria; the
402 formation of heterocysts (Nierzwicki-Bauer *et al.*, 1984a; Nierzwicki-Bauer *et al.*, 1984b;
403 Stevens *et al.*, 1985) and necridia (this study) seem to follow no regular spacing and distribution
404 pattern. Our analyses of the different types of branches also suggest a degree of randomness in

cell development. We hypothesise that "T" and "Y" branches are basically equivalent: the different forms simply result from loose control of the positioning of the cell elongation machinery.

As a possible component of the cell-cell connecting structures we identified SepJ. The protein consists of the typical three domain architecture found in other filamentous, heterocyst-forming cyanobacteria (Section IV), and immunofluorescence labelling revealed its localisation at the septa. A cell in the branching point exhibits three SepJ spots, suggesting that although *M. laminosus* shows branching, the septa are similar to those described in *Anabaena* sp. PCC 7120.

Earlier studies had suggested that rounded cells in wide trichomes are completely separated by their surrounding sheath (Thurston and Ingram, 1971; Martin and Wyatt, 1974; Nierzwicki *et al.*, 1982) which would imply a lack of communication between these cells. According to our ultrastructural and FRAP analyses this is however not the case. *M. laminosus* shows intercellular communication and highly-structured cell junctions between cells of various shapes, forming a complex network of cell communication. The hypothesis that cyanobacteria of Section V represent a primitive and basic form linking coccoid and filamentous forms (Martin and Wyatt, 1974), is not supported by our study. Our results from cell division and intercellular communication experiments indicate that Section V cyanobacteria are similar to cyanobacteria of Section IV. Section IV and V cyanobacteria show the highest degree of morphological complexity and diversity within the phylum.

Experimental Procedures

Organism, medium, and growth.

Mastigocladus laminosus SAG 4.84 was originally isolated by G. H. Schwabe from a thermal spring of Reyhjanes/Isafjord, Iceland in 1967. The cyanobacterium was grown in liquid Castenholz D medium (Castenholz, 1988) at 40°C, under constant white light at approximately 20 µE m^{-2} s^{-1}. To provide constant agitation cultures were bubbled with sterile air or shaken (100 rpm). For studies of intercellular communication between branch and main trichome, a resting culture was used to inoculate Castenholz D medium. After 24 h of growth cultures were loaded with 5-CFDA, and its transfer demonstrated by FRAP. Heterocyst differentiation was induced by growth for up to 96 h in Castenholz ND medium (Castenholz, 1988), which lacks combined nitrogen, under the above described conditions.

Labelling with fluorescent dyes.

For molecular exchange experiments, cells were labelled with the fluorescent tracers 5-carboxyfluorescein diacetate (5-CFDA; Molecular Probes) or calcein (Molecular Probes). 1 ml of *M. laminosus* culture was harvested by centrifugation (3000xg, 2 min.), washed twice and resuspended in 1 ml fresh growth medium, and mixed with 12 µl of a 1 mg ml^{-1} 5-CFDA or calcein, acetoxymethyl ester solution in dimethylsulphoxide. The suspension with 5-CFDA was incubated for 30 min at 40°C in the dark with shaking in an orbital incubator at 80 rpm, and the suspension with calcein for 90 min under the same conditions. To remove the fluorescent dyes, the cells were washed three times in growth medium, and incubated for another 30 min in 1 ml of medium at 40°C in the dark under gentle shaking (80 rpm). After a final washing step, cells were spotted onto a Castenholz D 1.5 % (w/v) agar plate, and excess solution was removed. To maintain the growth conditions throughout the experiment media and plates were preheated to 40°C.

Two additional fluorescent dyes, FM1-43FX and Hoechst 33258, were used to visualise specific cellular components. FM1-43FX stains the outer and cytoplasmic membranes of cyanobacteria (Schneider *et al.*, 2007), while Hoechst 33258 interacts with DNA. For labelling, we washed cells once in fresh growth medium, and added 1 µl Hoechst 33258 (1 mg ml^{-1}; Bisbenzimide H33258; AppliChem) and/or 2.5 µl FM1-43FX (0.1 mg ml^{-1}; Molecular Probes) to 0.5 ml of culture. The suspension was incubated for 10 min at room temperature and washed twice with growth medium prior mounting on 1.5 % (w/v) agar with Castenholz D or ND medium. Surplus medium was removed.

Confocal microscopy and Fluorescence Recovery after Photobleaching (FRAP).

For confocal microscopy, small blocks of agar were placed in a custom-built temperature-controlled sample holder covered with a glass cover slip. Cells were visualised with the Leica laser-scanning confocal microscope SP5 using a x63 oil-immersion objective (Leica HCX PL APO lambda blue 63.0x1.40 OIL UV), and an excitation wave length of 488 nm for 5-CFDA, calcein and FM1-43FX, and 355 nm for the Hoechst 33258-DNA complex. Chlorophyll *a* fluorescence (autofluorescence) and dye fluorescence were imaged simultaneously, using different emission detection ranges (455-495 nm for Hoechst 33258, 500-527 nm for 5-CFDA and calcein, 570-595 nm for FM1-43X, and 670-720 nm for the autofluorescence). For imaging, we used a 95 µm confocal pinhole, giving a resolution of 0.8 µm in the Z-direction (full width at half-maximum of the point-spread function), whereas we opened the pinhole maximal for FRAP measurements (600 µm, an optical section thickness of 4.2 µm respectively). After taking an initial image (pre-bleach), the region of interest (ROI) was bleached by increasing the laser intensity and zooming into the ROI, and recovery was recorded. Images were taken typically in 0.534 s intervals. FRAP data were analysed as described in (Mullineaux *et al.*, 2008) to estimate

the exchange coefficient E, using Image Pro Plus 6.3 (Media Cyberentics Inc.) and SigmaPlot 10.0 (Systat Software Inc.).

Electron Microscopy.

Cultures were harvested by centrifugation (3000x*g*; 2 min) and fixed for 2 h at room temperature with 4% (w/v) glutaraldehyde in 100 mM phosphate buffer pH 7.3. To remove the fixative, cells were washed three times with 100 mM phosphate buffer. After embedding in 2% (w/v) low-gelling temperature agarose, samples were cut in one- to two-millimetre cubic blocks, and post-fixed with 2% (w/v) potassium permanganate dissolved in distilled water over night at 4°C. Samples were washed with distilled water until the supernatant remained clear, and dehydrated through a graded ethanol series (1x15 min 30%, 1x15 min 50%, 1x15 min 70%, 1x15 min 90% and 3x20 min 100%). Two washes for 5min with propylene oxide were performed prior infiltration with Araldite for 1 h and with fresh Araldite over night. Polymerisation was achieved by incubation at 60-65°C for 48 h. Alternatively, cells were fixed for 2h at room temperature in 100 mM phosphate buffer pH 7.0 containing 3% (w/v) glutaraldehyde, 1% (w/v) formaldehyde and 0.5% (w/v) tannic acid, washed with phosphate buffer, and incubated in 2% (w/v) OsO_4 in phosphate buffer over night. Dehydration was performed using a graded acetone series as described for ethanol prior to embedding in Araldite. Thin sections were cut with a glass knife at a Reichert Ultracut E microtome and collected on uncoated, 300 mesh copper grids. High contrast was obtained by poststaining with saturated aqueous uranyl acetate and lead citrate (Reynolds, 1963) for 4 min each. The grids were examined in a JOEL JEM-1230 transmission electron microscope at an accelerating potential of 80kV.

DNA isolation, gene amplification, and sequencing.

Genomic DNA from *M. laminosus* was extracted using the protocol of Morin *et al*. (2010) with a cell homogenization step prior cell lysis. The cells were harvested by centrifugation (3,000x*g*, 5 min) and resuspended in fresh growth medium. Homogenization of the culture was achieved by multiple passages through a 0.8 mm needle with the help of a syringe. The cells were collected by centrifugation (3000x*g*, 5 min), and genomic DNA was isolated as previously described (Morin *et al.*, 2010)

To identify *sepJ* in *M. laminosus* oligonucleotide primers were designed as follows: Since there were no *sepJ* sequences known from *M. laminosus* and other species of Section V, we assumed a similarity in its sequence and localisation to other filamentous, heterocyst-forming cyanobacteria. *sepJ* nucleotide sequences from *Anabaena* sp. PCC 7120, *Anabaena variabilis* ATCC 29413, '*Nostoc azollae*' 0708 and *Nostoc punctiforme* PCC 73102 were obtained from the NCBI GenBank and aligned with Clustal W 2.1 (Larkin *et al.*, 2007). The first 20 nucleotides built primer fw_mlam_sepJ (5'-atggggcgatttgagaagcg-3') (Fig. S2B). The reverse primer was designed on the assumption that *hetR* is located downstream of *sepJ*. Available partial *hetR* sequences from cyanobacteria of Section V (*Fischerella* spp. and *Chlorogloeopsis* spp.) were used for a Clustal W 2.1 alignment, and resulted in primer rev_mlam_hetR (5'-gttgcggctgcatctaaaaa-3') (Fig. S2A).

The optimal annealing temperature for *sepJ* amplification was determined by using a gradient PCR with the Promega PCR Master Mix. PCR products were resolved by electrophoresis in a 1% (w/v) agarose gel. The final amplification was performed with the Roche Expand High Fidelity PCR System using the following conditions for a 50µl reaction: 94°C for 2 min, 15x cycle 1 (94°C for 45 sec; 48.9°C for 45 sec; 72°C for 4 min), 15x cycle 2 (94°C for 45 sec; 59°C for 45 sec; 72°C for 4 min) and 1x cycle 3 (94°C for 45 sec; 57°C for 45 sec; 72°C for 10 min).

516 The amplified product was checked on a 1% (w/v) agarose gel, and purified with the QIAquick
517 PCR purification kit (QIAGEN) for sequencing.

518 **Nucleotide sequence accession number.**

519 The identified *sepJ* sequence has been deposited in the GenBank database under the accession
520 number KF729033.

521 **Sequence analysis.**

522 The *sepJ* DNA sequence was translated into the corresponding amino acid sequence using the
523 ExPASy translate tool (http://web.expasy.org/translate/). A BlastP search was performed in order
524 to identify orthologous sequences (Altschul *et al.*, 1997). Further sequence analyses were
525 performed using the TMHMM server 2.0 (http://www.cbs.dtu.dk/services/TMHMM/) in order to
526 predict the localisation of transmembrane helices, TRUST (Szklarczyk and Heringa, 2004) for
527 the detection of internal repeats, and Coils/PCoils (http://toolkit.tuebingen.mpg.de/pcoils) for the
528 identification of potential coiled-coiled regions in SepJ.

529 **Immunofluorescence labelling and sample examination.**

530 Cells were harvested by centrifugation (3000x*g*; 2 min) and resuspended in fresh growth medium.
531 Cultures were transferred onto 0.2 µm Nucleopore membranes, which were subsequently placed
532 onto poly-L-lysine coated slides. For fixation the slides were incubated in 50-ml plastic Falcon
533 tubes containing 70% (v/v) chilled (-20°C) ethanol for 30 min at -20°C. After 3 washing steps for
534 2 min with phosphate-buffered saline (PBS: 137 mM NaCl, 2.7 mM KCl, 10 mM phosphate
535 buffer) with 0.1 % (v/v) Tween 20 (PBST), the samples were immersed in 3% (w/v) milk
536 powder, diluted in PBST, and incubated for 15 min at room temperature. Afterwards, the slides
537 were directly incubated with the primary antibody, rabbit anti-*Anabaena* sp. PCC 7120 SepJ

(Mariscal *et al.*, 2011), diluted 1:250 in PBST, and stored for 3 h at 30°C in a moisture chamber. After incubation, the samples were washed three times in PBST for 2 min, and then incubated with the secondary antibody for 45 min at 30°C. The secondary antibody was an anti-rabbit immunoglobulin G conjugated with Alexa Fluor 488 (Invitrogen) diluted 1:500 in PBST. After final washing steps with PBST (3x 2 min), the slides were mounted with a cover slip using FluorSave™ Reagent (Calbiochem), and sealed with nail varnish.

Immunolabelled cells were examined with a Leica DM6000B fluorescence microscope, using an x63 oil-immersion objective and an ORCA-ER camera (Hamamatsu). Alexa Fluor 488 fluorescence was monitored using a fluorescein isothiocyanate (FITC) L5 filter (excitation, band-pass [BP] 480/40 filter; emission, BP 527/30 filter), and autofluorescence was monitored using a Texas Red TX2 filter (excitation, BP 560/40; emission, BP 645/75). Images were convolved with the Leica Application Suite Advanced Fluorescence software.

Acknowledgements

We are especially grateful to Karina Stucken for advice on identifying *sepJ*. Furthermore, we thank Graham McPhail and Petra Ungerer for their support in electron microscopy, and Igor Brown, Jiří Komárek, and Damir Viličić for providing literature on various topics.

This work was supported by a college studentship of Queen Mary University of London, and the College Central Research Fund. Work in Seville was supported by grant no. BFU2011-22762 from Plan Nacional de Investigación, Spain, co-financed by FEDER.

The authors declare no conflict of interest.

References

559 Altschul, S.F., Madden, T.L., Schäffer, A.A., Zhang, J., Zhang, Z., Miller, W., and Lipman, D.J. (1997)
560 Gapped BLAST and PSI-BLAST: a new generation of protein database search programs. *Nucl Acids Res*
561 **25**: 3389–3402.

562 Anagnostidis, K., and Komárek, J. (1990) Modern approach to the classification system of Cyanophytes.
563 5-Stigonematales. *Arch Hydrobiol Suppl Algol Stud* **59**: 1–73.

564 Balkwill, D.L., Nierzwicki-Bauer, S.A., and Stevens, S.E.J. (1984) Modes of cell division and branch
565 formation in the morphogenesis of the cyanobacterium *Mastigocladus laminosus*. *J Gen Microbiol* **130**:
566 2079–2088.

567 Bekker, A., Holland, H.D., Wang, P.-L., Rumble, D., Stein, H.J., Hannah, J.L., *et al.* (2004) Dating the
568 rise of atmospheric oxygen. *Nature* **427**: 117–20.

569 Benson, D.A., Karsch-Mizrachi, I., Lipman, D.J., Ostell, J., and Sayers, E.W. (2011) GenBank. *Nucl*
570 *Acids Res* **39**: D32–D37.

571 Brown, I.I., Bryant, D.A., Casamatta, D., Thomas-Keprta, K.L., Sarkisova, S.A., Shen, G., *et al.* (2010)
572 Polyphasic characterization of a thermotolerant siderophilic filamentous cyanobacterium that produces
573 intracellular iron deposits. *Appl Env Microbiol* **76**: 6664–6672.

574 Buikema, W.J., and Haselkorn, R. (1991) Characterization of a gene controlling heterocyst differentiation
575 in the cyanobacterium *Anabaena* 7120. *Genes Dev* **5**: 321–330.

576 Butler, R.D., and Allsopp, A. (1972) Uhrastruetural investigations in the Stigonemataceae (Cyanophyta).
577 *Arch Microbiol* **82**: 283–299.

578 Campbell, E.L., and Meeks, J.C. (1989) Characteristics of hormogonia formation by symbiotic *Nostoc*
579 spp. in response to the presence of *Anthoceros punctatus* or its extracellular products. *Appl Env Microbiol*
580 **55**: 125–131.

581 Castenholz, R.W. (1976) The effect of sulfide on the bluegreen algae of hot springs. New Zealand and
582 Iceland. *J Phycol* **12**: 54–68.

583 Castenholz, R.W. (1988) Culturing methods for cyanobacteria. *Methods Enzymol* **167**: 68–93.

584 Cohn, F. (1862) Über die Algen des Karlsbader Sprudels, mit Rücksicht auf die Bildung des
585 Sprudelsinsters. *Abhandlungen der schlesischen Gesellschaft für vaterländische Kultur* **5**: 37–55.

586 Croft, W.N., and George, E.A. (1959) Blue-green algae from the Middle Devonian of Rhynie,
587 Aberdeenshire. *Bull Br Museum Nat Hist Geol* 341–353.

588 Dagan, T., Roettger, M., Stucken, K., Landan, G., Koch, R., Major, P., *et al.* (2013) Genomes of
589 stigonematalean cyanobacteria (Subsection V) and the evolution of oxygenic photosynthesis from
590 prokaryotes to plastids. *Genome Biol Evol* **5**: 31–44.

591 Desikachary, T. V (1959) *Cyanophyta*. Indian Council of Agricultural Research, New Delhi, India.

592 Finsinger, K., Scholz, I., Serrano, A., Morales, S., Uribe-lorio, L., Mora, M., *et al.* (2008) Characterization
593 of true-branching cyanobacteria from geothermal sites and hot springs of Costa Rica. *Env Microbiol* **10**:
594 460–473.

595 Flores, E., and Herrero, A. (2010) Compartmentalized function through cell differentiation in filamentous
596 cyanobacteria. *Nat Rev Microbiol* **8**: 39–50.

597 Flores, E., Pernil, R., Muro-Pastor, A.M., Mariscal, V., Maldener, I., Lechno-Yossef, S., *et al.* (2007)
598 Septum-localized protein required for filament integrity and diazotrophy in the heterocyst-forming
599 cyanobacterium *Anabaena* sp. strain PCC 7120. *J Bacteriol* **189**: 3884–3890.

600 Fogg, G.E., Stewart, W.D.P., Fay, P., and Walsby, A.E. (1973) *The Blue-Green Algae.* Academic Press,
601 London and New York.

602 Geitler, L. (1960) *Schizophyzeen.* Gebrüder Borntraeger, Berlin-Nikolassee, Germany.

603 Giddings, T.H.J., and Staehelin, L.A. (1978) Plasma membrane architecture of *Anabaena cylindrica*:
604 occurence of microplasmodesmata and changes associated with heterocyst development and the cell cycle.
605 *Cytobiologie* **16**: 235–249.

606 Giddings, T.H.J., and Staehelin, L.A. (1981) Observation of microplasmodesmata in both heterocyst-
607 forming and non-heterocyst forming filamentous cyanobacteria by freeze-fracture electron microscopy.
608 *Arch Microbiol* **129**: 295–298.

609 Golubić, S., Hernandez-Marine, M., and Hoffmann, L. (1996) Developmental aspects of branching in
610 filamentous Cyanophyta/Cyanobacteria. *Arch Hydrobiol Suppl Algol Stud* **83**: 303–329.

611 Hernandez-Muniz, W., and Stevens, S.E.J. (1987) Characterization of the motile hormogonia of
612 *Mastigocladus laminosus*. *J Bacteriol* **169**: 218–223.

613 Kohl, F.G. (1903) *Über die 0rganisation und Physiologic der Cyanophyeeenzelle und die mitotische*
614 *Teilung ihres Kernes.* Gustav Fischer, Jena, Germany.

615 Komárek, J., and Anagnostidis, K. (1989) Modern approach to the classification system of cyanophytes.
616 4-Nostocales. *Algol Stud* **56**: 247–345.

617 Komárek, J., Kling, H., and Komárková, J. (2003) Filamentous cyanobacteria. In *Freshwater Algae of*
618 *North America*. Wehr, J.D., and Sheath, R.G. (eds). Elsevier Inc., pp. 117–196.

619 Konhauser, K.O., Lalonde, S. V, Planavsky, N.J., Pecoits, E., Lyons, T.W., Mojzsis, S.J., *et al.* (2011)
620 Aerobic bacterial pyrite oxidation and acid rock drainage during the Great Oxidation Event. *Nature* **478**:
621 369–373.

622 Lamont, H.C. (1969) Sacrificial cell death and trichome breakage in an Oscillatoriacean blue-green alga:
623 the role of murein. *Arch Microbiol* **69**: 237–259.

624 Larkin, M.A., Blackshields, G., Brown, N.P., Chenna, R., McGettigan, P. a, McWilliam, H., *et al.* (2007)
625 Clustal W and Clustal X version 2.0. *Bioinformatics* **23**: 2947–2948.

Lehner, J., Berendt, S., Dörsam, B., Pérez, R., Forchhammer, K., and Maldener, I. (2013) Prokaryotic multicellularity: a nanopore array for bacterial cell communication. *FASEB J* **27**: 1–8.

Lockau, W., and Ziegler, K. (2006) Cyanophycin Inclusions: Biosynthesis and Applications. In *Microbial Bionanotechnology: Biological Self-Assembly Systems and Biopolymer-Based Nanostructures*. Rehm, B. (ed.). Horizon Scientific Press, pp. 79–106.

Mackenzie, R., Pedrós-Alió, C., and Díez, B. (2013) Bacterial composition of microbial mats in hot springs in Northern Patagonia: variations with seasons and temperature. *Extremophiles* **17**: 123–36.

Marcenko, E. (1962) Licht- und elektronenmikroskopische Untersuchungen an der Thermalalge *Mastigocladus laminosus* Cohn. *Acta Bot Coratica* **20/21**: 47–74.

Mariscal, V., Herrero, A., Nenninger, A., Mullineaux, C.W., and Flores, E. (2011) Functional dissection of the three-domain SepJ protein joining the cells in cyanobacterial trichomes. *Mol Microbiol* **79**: 1077–1088.

Markowitz, V.M., Chen, I.-M.A., Palaniappan, K., Chu, K., Szeto, E., Grechkin, Y., *et al.* (2012) IMG: the Integrated Microbial Genomes database and comparative analysis system. *Nucl Acids Res* **40**: D115–D122.

Martin, T.C., and Wyatt, J.T. (1974) Comparative physiology and morphology of six strains of Stigonematacean blue-green algae. *J Phycol* **10**: 57–65.

Meeks, J.C., Campbell, E.L., Summers, M.L., and Wong, F.C. (2002) Cellular differentiation in the cyanobacterium *Nostoc punctiforme*. *Arch Microbiol* **178**: 395–403.

Melick, D.R., Broady, P.A., and Rowan, K.S. (1991) Morphological and physiological characteristics of a non-heterocystous strain of the cyanobacterium *Mastigocladus laminosus* Cohn from fumarolic soil on Mt Erebus , Antarctica. *Polar Biol* 81– 89.

Merino-Puerto, V., Mariscal, V., Mullineaux, C.W., Herrero, A., and Flores, E. (2010) Fra proteins influencing filament integrity, diazotrophy and localization of septal protein SepJ in the heterocyst-forming cyanobacterium *Anabaena* sp. *Mol Microbiol* **75**: 1159–70.

Merino-Puerto, V., Schwarz, H., Maldener, I., Mariscal, V., Mullineaux, C.W., Herrero, A., and Flores, E. (2011) FraC/FraD-dependent intercellular molecular exchange in the filaments of a heterocyst-forming cyanobacterium, *Anabaena* sp. *Mol Microbiol* **82**: 87–98.

Miller, S.R., Purugganan, M.D., and Curtis, S.E. (2006) Molecular Population Genetics and Phenotypic Diversification of Two Populations of the Thermophilic Cyanobacterium *Mastigocladus laminosus*. *Appl Env Microbiol* **72**: 2793–2800.

Morin, N., Vallaeys, T., Hendrickx, L., Natalie, L., and Wilmotte, A. (2010) An efficient DNA isolation protocol for filamentous cyanobacteria of the genus *Arthrospira*. *J Microbiol Methods* **80**: 148–154.

Mullineaux, C.W., Mariscal, V., Nenninger, A., Khanum, H., Herrero, A., Flores, E., and Adams, D.G. (2008) Mechanism of intercellular molecular exchange in heterocyst-forming cyanobacteria. *EMBO J* **27**: 1299–1308.

Nayar, A.S., Yamaura, H., Rajagopalan, R., Risser, D.D., and Callahan, S.M. (2007) FraG is necessary for filament integrity and heterocyst maturation in the cyanobacterium *Anabaena* sp. strain PCC 7120. *Microbiology* **153**: 601–607.

Nierzwicki, S.A., Maratea, D., Balkwill, D.L., Hardie, L.P., Mehta, V.B., and Stevens, S.E.J. (1982) Ultrastructure of the cyanobacterium, *Mastigocladus laminosus*. *Arch Microbiol* **133**: 11 – 19.

Nierzwicki-Bauer, S.A., Balkwill, D.L., and Stevens, S.E.J. (1984a) Heterocyst differentiation in the cyanobacterium *Mastigocladus laminosus*. *J Bacteriol* **157**: 514–525.

Nierzwicki-Bauer, S.A., Balkwill, D.L., and Stevens, S.E.J. (1984b) Morphology and ultrastructure of the cyanobacterium *Mastigocladus laminosus* growing under nitrogen-fixing conditions. *Arch Microbiol* **137**: 97–103.

Pankratz, H.S., and Bowen, C.C. (1963) Cytology of Blue-Green Algae. I. The Cells of *Symploca muscorum*. *Amer J Bot* **50**: 387–399.

Reynolds, E.S. (1963) The use of lead citrate at high pH as an electron-opaque stain in electron microscopy. *J Cell Biol* **17**: 208–212.

Rippka, R., Deruelles, J., Waterbury, J.B., Herdman, M., and Stanier, R.Y. (1979) Generic assignments, strain histories and properties of pure cultures of cyanobacteria. *J Gen Microbiol* **111**: 1–61.

Robinson, W.B., Mealor, A.E., Stevens, S.E.J., and Ospeck, M. (2007) Measuring the force production of the hormogonia of *Mastigocladus laminosus*. *Biophys J* **93**: 699–703.

Schirrmeister, B.E., Anisimova, M., Antonelli, A., and Bagheri, H.C. (2011) Taxa required for improved phylogenomic approaches. *BMC Evol Biol* **4**: 424–427.

Schneider, D., Fuhrmann, E., Scholz, I., Hess, W.R., and Graumann, P.L. (2007) Fluorescence staining of live cyanobacterial cells suggest non-stringent chromosome segregation and absence of a connection between cytoplasmic and thylakoid membranes. *BMC Cell Biol* **10**: 1–10.

Schwabe, G.H. (1960) Über den thermobionten Kosmopoliten *Mastigocladus laminosus* Cohn. *Hydrology* 759–792.

Shih, P.M., Wu, D., Latifi, A., Axen, S.D., Fewer, D.P., Talla, E., *et al.* (2013) Improving the coverage of the cyanobacterial phylum using diversity-driven genome sequencing. *Proc Natl Acad Sci USA* **110**: 1053–1058.

Singh, R.N., and Tiwari, D.N. (1969) Induction by Ultraviolet Irradiation of Mutation in the Blue-Green Alga *Nostoc linckia* (Roth) Born. et Flah. *Nature* **221**: 62–64.

Smith, D.J., Timonen, H.J., Jaffe, D. a, Griffin, D.W., Birmele, M.N., Perry, K.D., *et al.* (2013) Intercontinental dispersal of bacteria and archaea by transpacific winds. *Appl Env Microbiol* **79**: 1134–1139.

Soe, K.M., Yokoyama, A., Yokoyama, J., and Hara, Y. (2011) Morphological and genetic diversity of the thermophilic cyanobacterium, *Mastigocladus laminosus* (Stigonematales, Cyanobacteria) from Japan and Myanmar. *Phycol Res* **59**: 135–142.

Stevens, S.E.J., Nierzwicki-Bauer, S.A., and Balkwill, D.L. (1985) Effect of nitrogen starvation on the morphology and ultrastructure of the cyanobacterium *Mastigocladus laminosus*. *J Bacteriol* **161**: 1215–8.

Szklarczyk, R., and Heringa, J. (2004) Tracking repeats using significance and transitivity. *Bioinformatics* **20**: 311–317.

Thurston, E.L., and Ingram, L.O. (1971) Morphology and fine structure of Fischerella ambigua. *J Phycol* **7**: 203–210.

Tomitani, A., Knoll, A.H., Cavanaugh, C.M., and Ohno, T. (2006) The evolutionary diversification of cyanobacteria: molecular-phylogenetic and paleontological perspectives. *Proc Natl Acad Sci USA* **103**: 5442–5447.

Wildon, D.C., and Mercer, F. V (1963) The ultrastructure of the vegetative cell of blue-green algae. *Aust J Biol Sci* **16**: 585–596.

Wilk, L., Strauss, M., Rudolf, M., Nicolaisen, K., Flores, E., Kühlbrandt, W., and Schleiff, E. (2011) Outer membrane continuity and septosome formation between vegetative cells in the filaments of *Anabaena* sp . PCC 7120. *Cell Microbiol* **49**: 1–12.

Zhang, J.-Y., Chen, W.-L., and Zhang, C.-C. (2009) hetR and patS , two genes necessary for heterocyst pattern formation , are widespread in filamentous nonheterocyst-forming cyanobacteria. *Microbiology* **155**: 1418–1426.

716

Table 1. Exchange (E) and flux coefficients (F) for 5-CFDA in *M. laminosus.*

measurement	**mean E [s^{-1}] (± s.d.)**	**mean F [$\mu m^3 s^{-1}$] (± s.d.)**
1. cells in narrow trichomes	0.159 ± 0.072	7.65 ± 5.19
2. cells in wide trichomes	0.058 ± 0.044	3.60 ± 2.47
3. cells in hormogonia	0.132 ± 0.063	3.14 ± 1.04

t-tests indicate that E and F are significantly different in (1) and (2) ($P<0.00001$). Number of experiments performed for (1) 27, (2) 57, and (3) 9

Figure Legends

FIG.1. Different types of branching in *M. laminosus*, and their development revealed by confocal (A,B,D) and transmission electron microscopy (C). Two main types of branching are present in *M. laminosus*, namely (reverse) "Y"- (A) and "T"-branching (B). While the division plane is localised parallel to the main filament axis in "T"-branching (B), it remains nearly transversal to the main filament axis during the formation of a (reverse) "Y"-branch (A,C). Cells at the terminus of the main trichome grow into the direction of the main filament but alter their cell shape (D). A,B. The images show FM1-43 FX fluorescence (yellow; left), chlorophyll *a* fluorescence (magenta, middle), and an overlay of both (right). Scale bars, 5µm. C. Electron micrograph of a thin section prepared with $KMnO_4$; scale bar, 2µm. D. Bright-field image; scale bar, 5µm.

FIG. 2. Intercellular transfer of 5-CFDA between branch and main trichome in a "T"-branch of *M. laminosus*. A. FRAP image sequence. Only 5-CFDA fluorescence is shown. The left image was recorded prior to bleaching (pre). After bleaching out fluorescence in the branch (t = 0), the change in fluorescence intensity was followed over 32 s. Scale bars, 5 µm. B. Quantitation of cell fluorescence of the FRAP sequence displayed in A. Regions of interest (ROI) were defined as shown in the left image, the "T"-branch comprised of three cells was considered as one ROI ("cell 3"). The corresponding fluorescence recovery is indicated in the right graph. Scale bar, 5 µm.

FIG. 3. Electron micrographs of ultra thin sections through the septal region of *M. laminosus*, and localisation of SepJ by immunofluorescent labelling. A,B. Electron micrographs indicate the presence of structures connecting the cytoplasm of adjacent cells (septosomes; arrows) in *M.*

laminosus, using either a $KMnO_4$- (A) or a OsO_4-based preparation method (B). Septosomes are present between vegetative cells (A), and between vegetative cells and heterocysts (B). Note that the outer membrane does not enter the septum. CP – cyanophycin plug. Scale bars, 200nm. C. Localisation of SepJ in *M. laminosus* by immunofluorescent labelling. SepJ is localised in distinct spots in the septa between two adjacent vegetative cells. A branching point shows three distinct regions where SepJ is present (arrow). The images show SepJ immunolabelling (green; left), fluorescence of chlorophyll *a* (magenta; middle), and an overlay of both (right). Scale bars, 5µm.

FIG. 4. Position of heterocysts in filaments of *M. laminosus*. A-D. Heterocysts (arrows) can be found either in the branching start of "T"- (A) or (reverse) "Y"-branches (C), or in the new formed lateral branches (B and D, respectively). Note the position of cyanophycin granules in the heterocysts. They are always located close to cells they are connected with. Scale bars, 5 µm. E. Double heterocyst in a narrow trichome of *M. laminosus* (arrows). Cyanophycin granules are located at each pole of the cell, resulting in two cyanophycin plugs between two heterocysts. Scale bar, 10 µm. F. Electron micrograph of an ultra-thin section of a heterocyst in *M. laminosus*. A cyanophycin plug (CP) is present in the neck region. Rearrangements of thylakoid membranes are visible. The sample was prepared using the $KMnO_4$ method. Scale bar, 1µm.

FIG. 5. Function of necridia in intercellular communication, and their localisation in filaments of *M. laminosus*. A. FRAP image sequence of 5-CFDA loaded cells. Intercellular transfer is inhibited between main trichome and branch by the formation necridium (grey arrow).The left image was recorded prior to bleaching (pre). After bleaching out fluorescence in the branch (t = 0), recovery was followed over 24 s. The ROI is indicated with a white arrow. Scale bars, 5µm.B-D. Position of necridia and reorganisation of membranes in filaments of *M. laminosus*. Necridia

(arrows) can be found in the branching start (B), at the beginning of a recently formed branch (C), or at various positions within a narrow trichome (D). Their position follows no regular pattern. Two necridia can be even found in a single filament, separated only by one vegetative cell (D).The images show FM1-43 FX fluorescence (yellow; left), autofluorescence (magenta, middle) and an overlay of both (right). Scale bars, 5 µm.

FIG. 6. Appearance of necridia after filament release. A. Localisation of DNA in a hormogonium of *M. laminosus*. DNA was visualised by staining cells with Hoechst 33258 (blue). Autofluorescence is shown in magenta. An overlay with the bright-field image illustrates the position of DNA in the hormogonium, while a dead part remains at the end of the released filament (arrow). Scale bars, 5µm. B. Electron micrograph of an ultra-thin section of a branch terminus after filament breakage via necridium formation. Note that plasma membrane (PM) and outer membrane (OM) are sealed at the terminal cell to prevent cell death by molecule efflux. The sample was prepared with the method based on $KMnO_4$. Scale bar, 1 µm.

Supporting Information

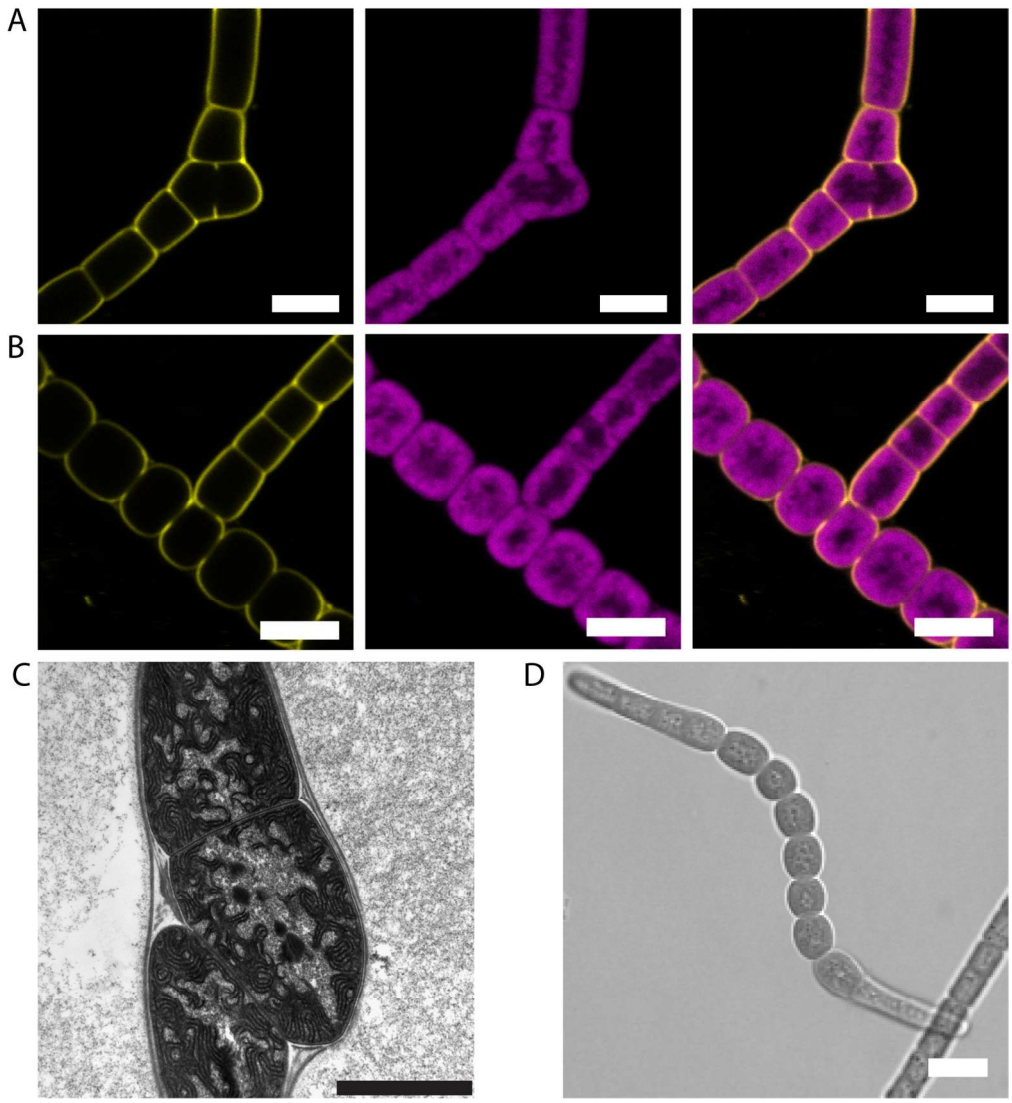

FIG.1. Different types of branching in M. laminosus, and their development revealed by confocal (A,B,D) and transmission electron microscopy (C). Two main types of branching are present in M. laminosus, namely (reverse) "Y"- (A) and "T"-branching (B). While the division plane is localised parallel to the main filament axis in "T"-branching (B), it remains nearly transversal to the main filament axis during the formation of a (reverse) "Y"-branch (A,C). Cells at the terminus of the main trichome grow into the direction of the main filament but alter their cell shape (D). A,B. The images show FM1-43 FX fluorescence (yellow; left), chlorophyll a fluorescence (magenta, middle), and an overlay of both (right). Scale bars, 5µm. C. Electron micrograph of a thin section prepared with KMnO4; scale bar, 2µm. D. Bright-field image; scale bar, 5µm.
149x163mm (300 x 300 DPI)

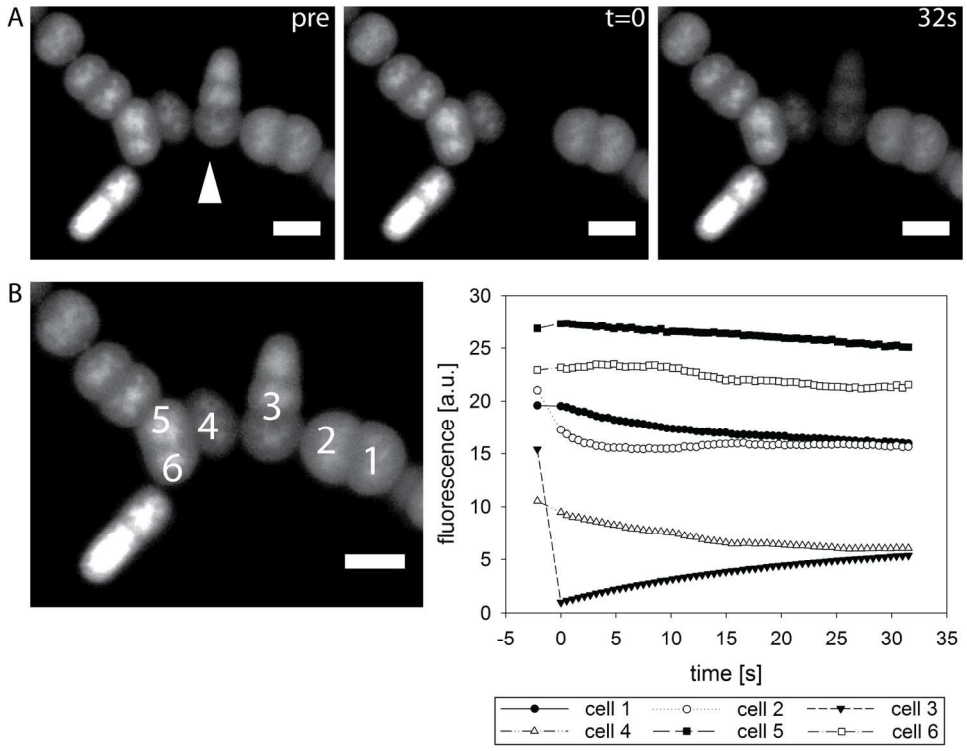

FIG. 2. Intercellular transfer of 5-CFDA between branch and main trichome in a "T"-branch of M. laminosus. A. FRAP image sequence. Only 5-CFDA fluorescence is shown. The left image was recorded prior to bleaching (pre). After bleaching out fluorescence in the branch (t = 0), the change in fluorescence intensity was followed over 32 s. Scale bars, 5 µm. B. Quantitation of cell fluorescence of the FRAP sequence displayed in A. Regions of interest (ROI) were defined as shown in the left image, the "T"-branch comprised of three cells was considered as one ROI ("cell 3"). The corresponding fluorescence recovery is indicated in the right graph. Scale bar, 5 µm.
151x112mm (300 x 300 DPI)

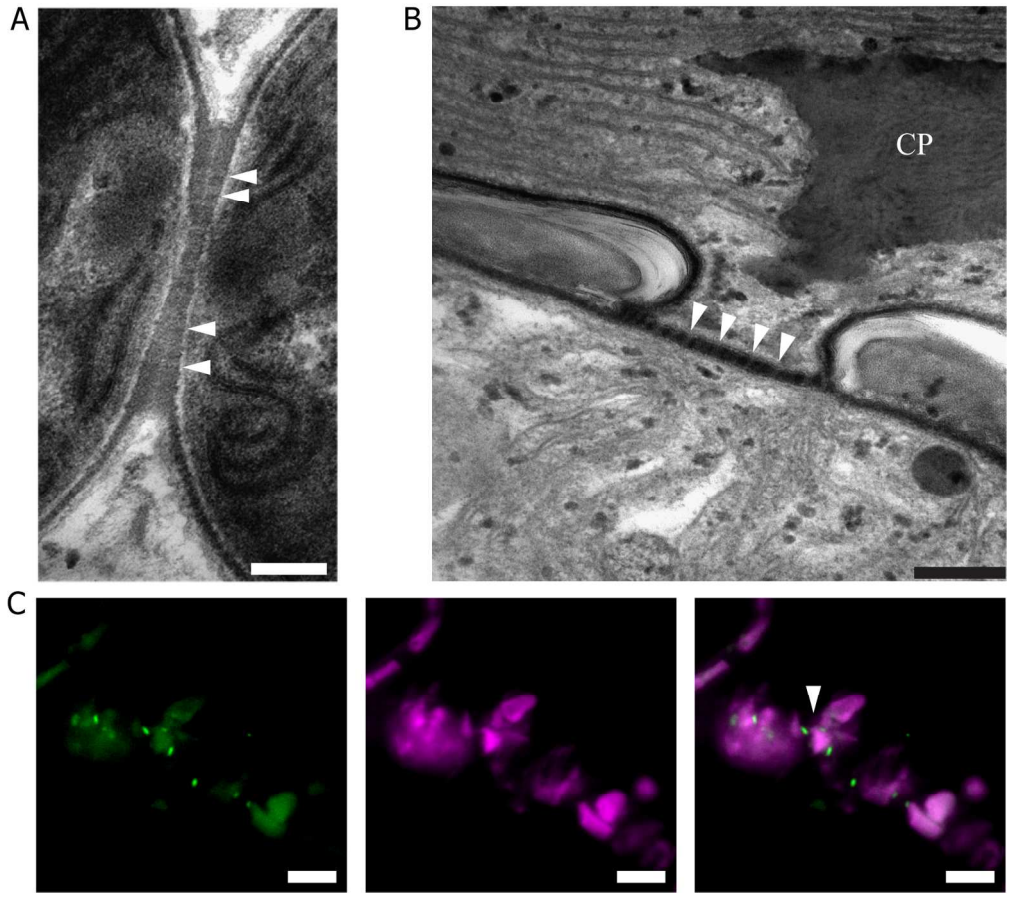

FIG. 3. Electron micrographs of ultra thin sections through the septal region of M. laminosus, and localisation of SepJ by immunofluorescent labelling. A,B. Electron micrographs indicate the presence of structures connecting the cytoplasm of adjacent cells (septosomes; arrows) in M. laminosus, using either a KMnO4- (A) or a OsO4-based preparation method (B). Septosomes are present between vegetative cells (A), and between vegetative cells and heterocysts (B). Note that the outer membrane does not enter the septum. CP – cyanophycin plug. Scale bars, 200nm. C. Localisation of SepJ in M. laminosus by immunofluorescent labelling. SepJ is localised in distinct spots in the septa between two adjacent vegetative cells. A branching point shows three distinct regions where SepJ is present (arrow). The images show SepJ immunolabelling (green; left), fluorescence of chlorophyll a (magenta; middle), and an overlay of both (right). Scale bars, 5µm.
158x140mm (300 x 300 DPI)

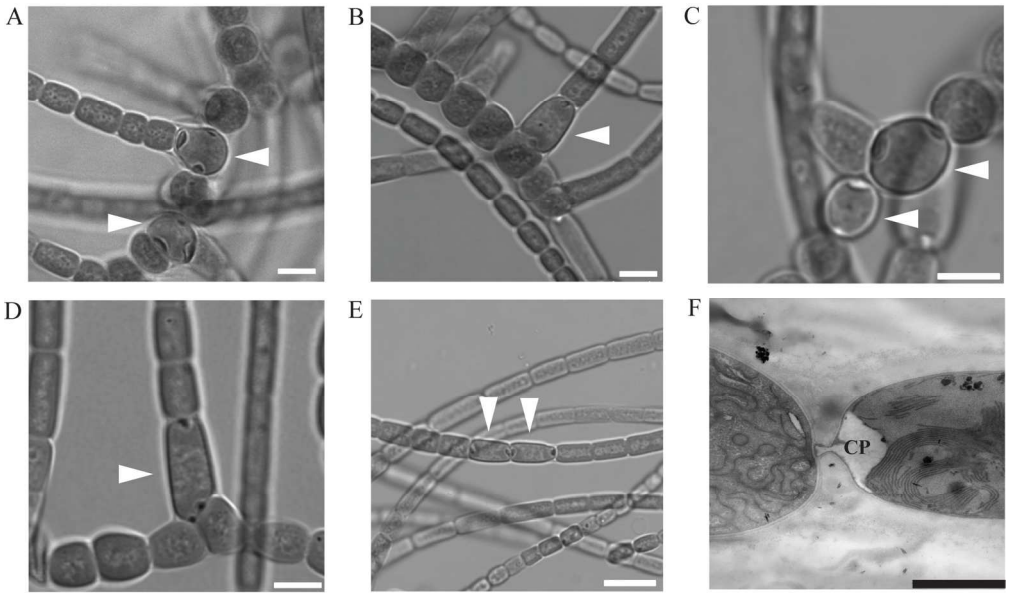

FIG. 4. Position of heterocysts in filaments of M. laminosus. A-D. Heterocysts (arrows) can be found either in the branching start of "T"- (A) or (reverse) "Y"-branches (C), or in the new formed lateral branches (B and D, respectively). Note the position of cyanophycin granules in the heterocysts. They are always located close to cells they are connected with. Scale bars, 5 µm. E. Double heterocyst in a narrow trichome of M. laminosus (arrows). Cyanophycin granules are located at each pole of the cell, resulting in two cyanophycin plugs between two heterocysts. Scale bar, 10 µm. F. Electron micrograph of an ultra-thin section of a heterocyst in M. laminosus. A cyanophycin plug (CP) is present in the neck region. Rearrangements of thylakoid membranes are visible. The sample was prepared using the KMnO4 method. Scale bar, 1µm.
168x99mm (300 x 300 DPI)

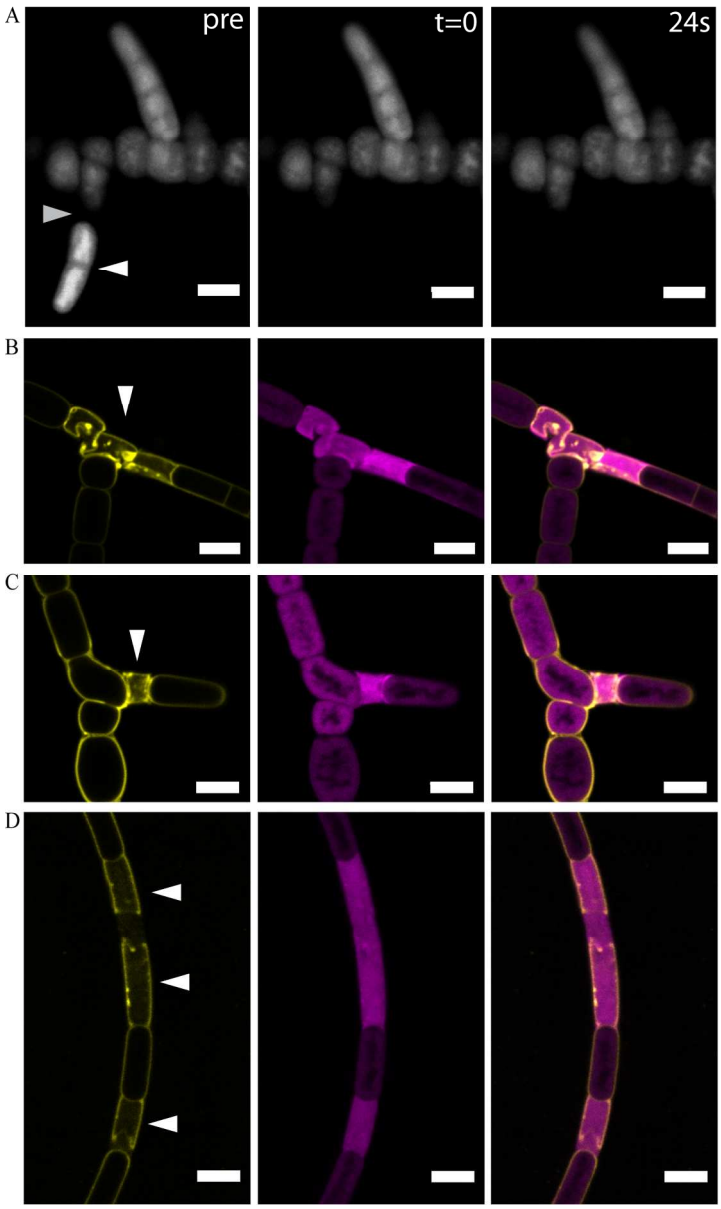

FIG. 5. Function of necridia in intercellular communication, and their localisation in filaments of M. laminosus. A. FRAP image sequence of 5-CFDA loaded cells. Intercellular transfer is inhibited between main trichome and branch by the formation necridium (grey arrow).The left image was recorded prior to bleaching (pre). After bleaching out fluorescence in the branch (t = 0), recovery was followed over 24 s. The ROI is indicated with a white arrow. Scale bars, 5µm.B-D. Position of necridia and reorganisation of membranes in filaments of M. laminosus. Necridia (arrows) can be found in the branching start (B), at the beginning of a recently formed branch (C), or at various positions within a narrow trichome (D). Their position follows no regular pattern. Two necridia can be even found in a single filament, separated only by one vegetative cell (D).The images show FM1-43 FX fluorescence (yellow; left), autofluorescence (magenta, middle) and an overlay of both (right). Scale bars, 5 µm.
135x225mm (300 x 300 DPI)

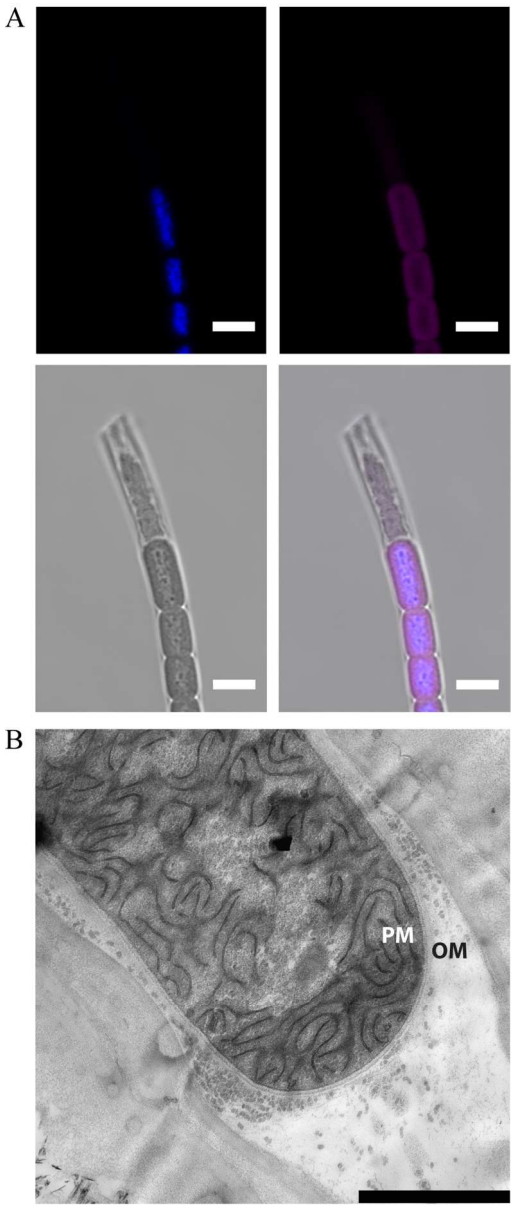

FIG. 6. Appearance of necridia after filament release. A. Localisation of DNA in a hormogonium of M. laminosus. DNA was visualised by staining cells with Hoechst 33258 (blue). Autofluorescence is shown in magenta. An overlay with the bright-field image illustrates the position of DNA in the hormogonium, while a dead part remains at the end of the released filament (arrow). Scale bars, 5μm. B. Electron micrograph of an ultra-thin section of a branch terminus after filament breakage via necridium formation. Note that plasma membrane (PM) and outer membrane (OM) are sealed at the terminal cell to prevent cell death by molecule efflux. The sample was prepared with the method based on KMnO4. Scale bar, 1 μm.
78x186mm (300 x 300 DPI)

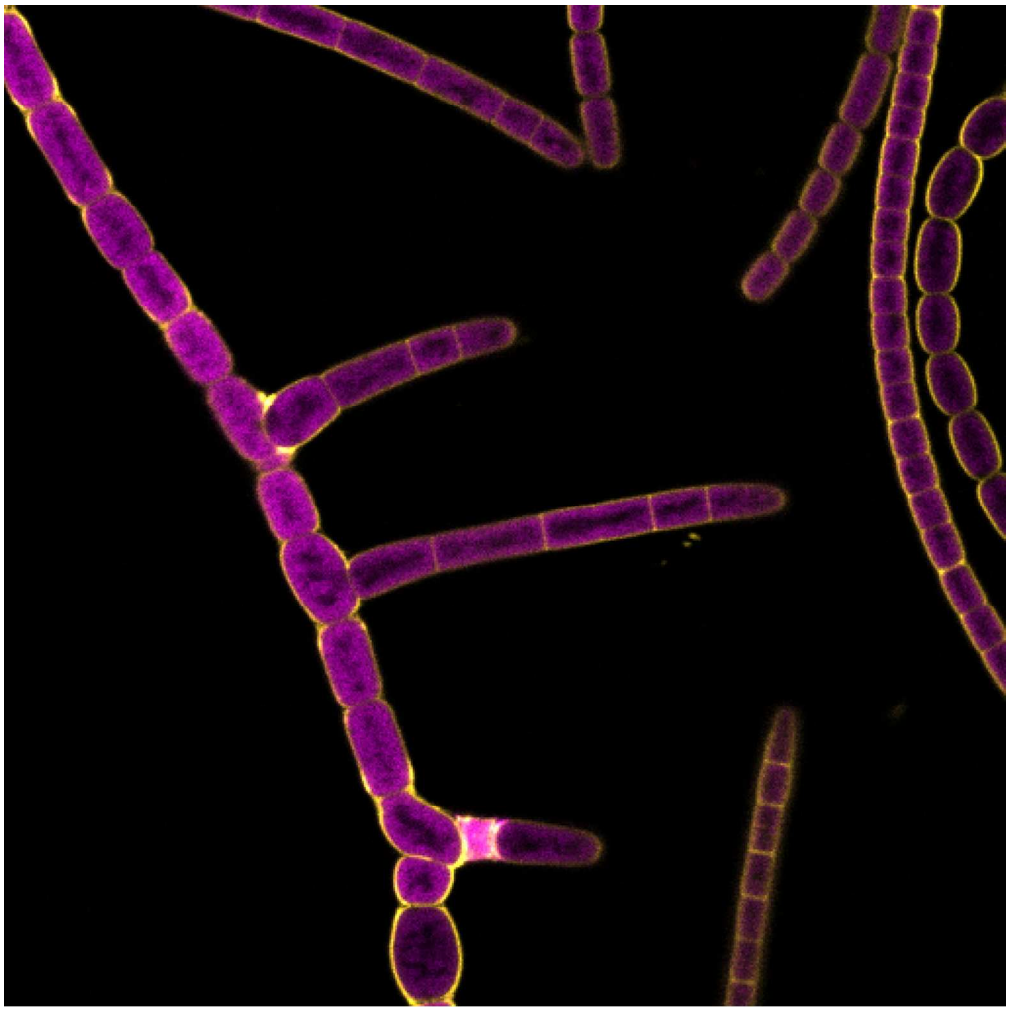

Fluorescence micrograph of the cyanobacterium Mastigocladus laminosus, showing different cell morphotypes exhibited by this complex prokaryote. Yellow: fluorescence from a cytoplasmic membrane stain; magenta: chlorophyll fluorescence.
135x135mm (300 x 300 DPI)